Polímeros
ISSN 1678-5169 (Online)

https://doi.org/10.1590/0104-1428.20240084

ORIGINAL ARTICLES

Development of green composites based on bio-polyethylene and babassu mesocarp

Crisnam Kariny da Silva Veloso[1], Lucas Rafael Carneiro da Silva[2], Ruth Marlene Campomanes Santana[2], Tatianny Soares Alves[1] and Renata Barbosa[1]*

[1]Programa de Pós-graduação em Ciência e Engenharia dos Materiais, Universidade Federal do Piauí, Teresina, PI, Brasil

[2]Programa de Pós-graduação em Engenharia de Minas, Metalúrgica e de Materiais, Universidade Federal do Rio Grande do Sul, Porto Alegre, RS, Brasil

***rrenatabarbosa@yahoo.com**

Abstract

Green composites are sustainable alternatives to conventional materials. This study developed composites based on bio-polyethylene (Bio-PE) and babassu mesocarp (BM) (1.5 and 3 phr), using PE-grafted maleic anhydride (PE-*g*-MA) (3 phr) as a compatibilizer. Materials were processed by extrusion and injection molding. BM exhibited starch-rich structure with a maximum degradation peak at 306 °C. PE-*g*-MA improved dispersion and surface finish, increasing the contact angle by up to 9.06%. Compared to neat Bio-PE, composites with PE-*g*-MA showed a 44.33% increase in yield stress and a 50.49% rise in ultimate tensile strength. Izod impact strength remained unchanged. Water absorption increased with BM, but was reduced up to 33.57% with PE-*g*-MA. This work introduces a novel use of BM in Bio-PE matrices, highlighting its potential as a Brazilian, renewable filler for sustainable composites.

Keywords: *compatibilization, contact angle, fracture surface morphology, mechanical properties, water absorption.*

Data Availability: Research data is available upon request from the corresponding.

How to cite: Veloso, C. K. S., Silva, L. R. C., Santana, R. M. C., Alves, T. S., & Barbosa, R. (2025). Development of green composites based on bio-polyethylene and babassu mesocarp. *Polímeros: Ciência e Tecnologia*, *35*(3), e20250032. https://doi.org/10.1590/0104-1428.20240084

1. Introduction

The demand for environmentally friendly materials has grown due to concerns about climate change, plastic waste, and resource scarcity[1]. This transition is supported by regulations on single-use plastics, consumer preference for sustainable materials, and industrial initiatives[2]. Green composites, which combine bio-based polymers with natural reinforcements, offer solutions aligned with the circular economy[3,4]. These materials aim to reduce pollution through biodegradability and renewable inputs while maintaining mechanical performance and cost-effectiveness[4,5].

Polyethylene (PE), widely used for its mechanical strength and chemical resistance, is fossil-based and contributes to environmental issues[4,5]. Bio-polyethylene (Bio-PE), derived from sugarcane ethanol, offers similar properties with reduced carbon emissions—up to 70% less than conventional PE[5,6]. However, concerns remain about land use, water consumption, and its non-biodegradability[7,8]. Incorporating natural fillers into Bio-PE can improve performance and reduce costs and environmental impact[3,5].

Several natural reinforcements have been successfully incorporated into Bio-PE to produce green composites. Dolza et al.[3] demonstrated that the incorporation of hemp, flax, and jute fibers into Bio-PE significantly improved the stiffness and thermal stability of the resulting composites. Rojas-Lema et al.[5] investigated the use of persimmon peel flour, which contributed to enhanced antioxidant capacity and reduced water absorption. Jorda-Reolid et al.[6] used argan shell waste in Bio-PE composites and observed increased rigidity and reduced material density. Despite these advances, babassu mesocarp (BM), a lignocellulosic material that is typically Brazilian, remains unexplored as a reinforcement in Bio-PE composites.

The babassu palm (*Attalea speciosa*), native to northern and northeastern Brazil, is socioeconomically important for local communities[9]. This palm produces a fruit with multiple layers (Figure 1), including the epicarp (outer shell), mesocarp (fibrous middle layer), endocarp (woody inner shell), and almonds, which are rich in oil and widely used in the food industry[10]. The mesocarp is a lignocellulosic material containing starch, fibers, and other minor components, making it a low-cost and underutilized residue with potential application in polymer composites[11,12]. Its incorporation into Bio-PE may reduce waste and promote sustainable material development. To date, no studies have investigated BM in Bio-PE composites, highlighting a research gap.

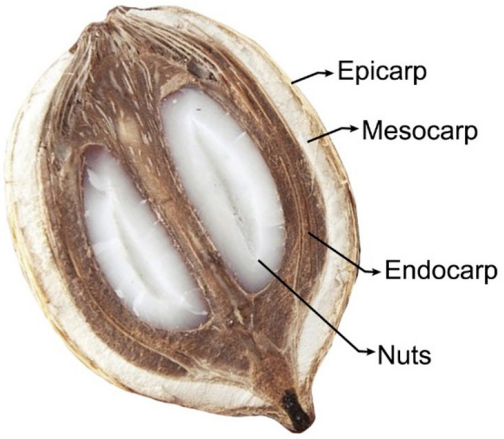

Figure 1. Morphological structure of babassu fruit.

Adding BM to Bio-PE can reduce petroleum-based content, enhance biodegradability, and improve cost-effectiveness[1,3]. However, its hydrophilic nature leads to compatibility issues with the hydrophobic polymer matrix, affecting mechanical and barrier properties[13]. Polyethylene-grafted maleic anhydride (PE-*g*-MA) has been widely used as a compatibilizer in natural filler composites and is a promising strategy to improve the compatibility between BM and the Bio-PE matrix by reducing phase separation and improving dispersion[6,14,15].

This study aims to develop composites combining Bio-PE and BM, using PE-*g*-MA to address compatibility challenges. The materials were characterized to evaluate the effects of BM and compatibilizer content on the properties of the composites. The use of BM as a Brazilian renewable filler in Bio-PE represents a novel approach for sustainable materials development.

2. Materials and Methods

2.1 Materials

Bio-Polyethylene (Bio-PE), grade SHC7260, with a minimum renewable source content of 94% (ASTM D6866) and suitable for injection processing, was used as the polymer matrix (Braskem, Brazil). It has a density of 0.959 g/cm^3, a melt flow index (MFI) of 7.2 g/10 min (190 °C/2.16 kg), and a glass transition temperature (T_g) similar to that of High-Density Polyethylene (HDPE) at around -100 °C[16]. Babassu Mesocarp (BM), a by-product of the babassu oil extraction industry (Florestas Brasileiras S.A., Itapecuru-Mirim, MA, Brazil), was used with an average particle diameter of 38.82 µm[10]. The compatibilizing agent was PE-*g*-MA, containing 1 wt% maleic anhydride, with a density of 0.954 g/cm^3, an MFI of 5 g/10 min (190 °C/2.16 kg), and a melting temperature (T_m) of 128 °C (Arkema, France).

2.2 Development of polymer composites based on Bio-PE/BM

Bio-PE, BM, and PE-*g*-MA were dried at 80 °C for 24 h, following the method described by Silva et al.[11]. Subsequently, the dried materials were manually mixed in specified proportions to produce various composite formulations, as detailed in Table 1.

Table 1. Formulations for Bio-PE/BM-based composites without and with the PE-*g*-MA.

Formulations	Content (phr)*		
	Bio-PE	BM	PE-*g*-MA
Bio-PE	100	0	0
Bio-PE/1.5BM	100	1.5	0
Bio-PE/3BM	100	3	0
Bio-PE/1.5BM/3PE-*g*-MA	100	1.5	3
Bio-PE/3BM/3PE-*g*-MA	100	3	3

*The content of BM and PE-*g*-MA was determined based on phr (parts per hundred resin).

The formulations were processed using a single-screw extruder (screw diameter: 16 mm, L/D ratio: 26) from AX Plásticos (Model AX-16), Brazil. The heating zones were set at 185, 190, and 195 °C, with a screw speed of 50 rpm. Under these conditions, the virgin Bio-PE pellets were processed to produce the control material. The extruded material was then cooled in water at room temperature (RT), pelletized, and stored for later use. A BM content of 3 wt% was employed due to its favorable processing properties, as higher contents present limitations. An injection molding machine (Model BL52, Eurostec, Brazil) was used to create specimens for tensile strength (ASTM D638) and Izod impact strength tests (ASTM D256). The heating zones were set to 185, 190, 200, and 200 °C from the feeding section to the nozzle, with a cycle time of 35 s, a mold temperature of 25 °C, and injection and holding pressures of 70 and 35 bar, respectively. Figure 2 depicts the entire process of developing Bio-PE/BM composites, from pellet production via extrusion to specimen creation through injection molding.

2.3 Characterizations

The Fourier-transform infrared spectroscopy (FTIR) spectrum was recorded using a PerkinElmer Spectrum 1000 spectrophotometer, covering a range from 4000 to 500 cm^{-1}. A BM sample was mixed with potassium bromide (KBr), pressed into a tablet, and analyzed using 32 scans at a resolution of 4 cm^{-1}. Thermogravimetric analysis for the BM was performed using a TA Instruments Q50 V20.13 Build 39 under a nitrogen atmosphere with a gas flow rate of 100 ml/min, a heating rate of 20 °C/min, and a final temperature of 900 °C.

The films' surface morphology was examined using a Leica DM500 binocular optical microscope in reflection mode, with an ICC50 E camera, 40x magnification, and 500 µm scale. The sessile drop method was employed to assess the contact angle (θ) of composites and determine their hydrophilic or hydrophobic nature. A 10 µl distilled water droplet was placed on the surface, and droplet images were captured using a 48-megapixel camera. The Surftens software (version 4.5) was then used to analyze these images and calculate the contact angle. The final contact angle value was obtained by averaging ten measurements for each composite.

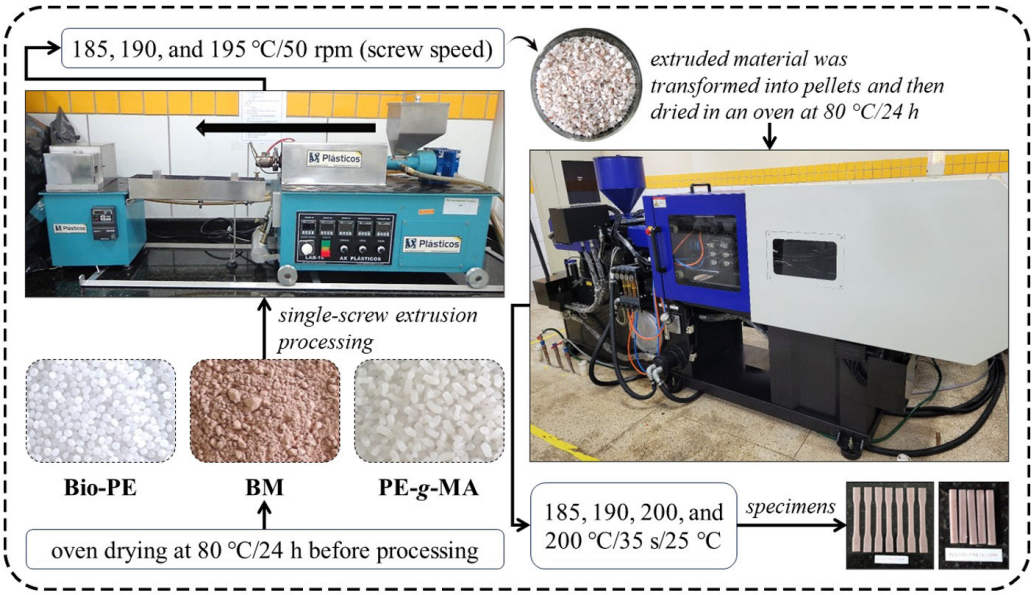

Figure 2. Schematic representation of the steps involved in the development of composites.

The tensile strength test was conducted using an EMIC DL 30000 Universal Testing Machine by ASTM D638 standards. A 5 kN load cell and a 50 mm/min crosshead speed were employed at RT. This test assessed the material's yield strength, ultimate tensile strength, and Young's modulus, representing the average of five specimens. The impact strength test was conducted using the Izod method on a CEAST Resil 5.5 J machine with a 2.75 J hammer at RT, according to ASTM D256. Specimens measuring 60 x 13 x 3.2 mm were notched to a depth of 2.5 mm. The final result corresponded to the average of five specimens.

After the tensile strength test, the fracture morphology was analyzed using gold-coated specimens with a scanning electron microscope (Model VEGA3, TESCAN) set to 20 kV. Micrographs were captured at 200 and 100 µm scale. ASTM D570 standard guided the water absorption test, during which five specimens were submerged in distilled water at RT, 50 °C, and 70 °C. A digital water bath (Model SL-150, Solab, Brazil) was used for heating. The specimens were weighed after 2, 24, 48, and 72 h, following the removal of excess water, using an analytical balance with an accuracy of 0.0001 g. The water content was calculated based on the mass difference, and the specimens were re-submerged after each weighing.

The data were analyzed using one-way ANOVA and compared between pairs of means with the Tukey test at a 5% significance level ($p < 0.05$) using OriginPro software (version 9.8).

3. Results and Discussions

3.1 Fourier Transform Infrared Spectroscopy (FTIR)

The FTIR technique reveals molecular vibrations by detecting how chemical bonds absorb infrared radiation at specific wavenumbers, thereby aiding in identifying functional groups within a material.

The FTIR spectrum demonstrated that the BM (Figure 3) closely resembles various starches due to its high starch content[12]. Critical absorption bands include 3333 cm^{-1} for −OH stretching, which is influenced by hydrogen bonding and free water; 2930 cm^{-1} for $-CH_2$ and $-CH_3$ vibrations from fatty acids; and 1646 cm^{-1} for hydroxyl groups of absorbed water[17,18]. Additional bands at 1426 and 1372 cm^{-1} indicated C−H bending in polysaccharides, while bands at 1160, 1079, 1014, 931, 861, and 763 cm^{-1} correspond to various C−O, C−C, and C−H vibrations in starch[19,20].

3.2 Thermogravimetric Analysis (TGA)

The TGA technique assessed the thermal stability of BM, as depicted in Figure 4. The TG and DTG curves revealed three decomposition stages.

The first stage, occurring at 75.30 and 81.37 °C, involved a mass loss of 2.64% due to water evaporation. The second stage, between 277.93 and 335.61 °C, was the main thermal event, showing a mass loss of 72.84% linked to the decomposition of carbohydrates, lipids, and proteins[21]. DTG curve highlighted a peak at 306.30 °C, indicating maximum decomposition temperature. The third stage, occurring from 335.61 to 902.36 °C, resulted in a mass loss of 10.56%, associated with the decomposition of other molecules, leaving a 13.22% residue (probably minerals)[14]. The results obtained are consistent with previous studies that analyzed the thermal decomposition of biomaterials rich in polysaccharides. Silva et al.[11] and Edvan et al.[21] observed that the thermal degradation of babassu mesocarp occurs mainly between 250–350 °C, attributing this range to the decomposition of starch and cellulose.

3.3 Macroscopic analysis

The produced composites were visually analyzed, and images were captured to support the observations, as shown in Figure 5.

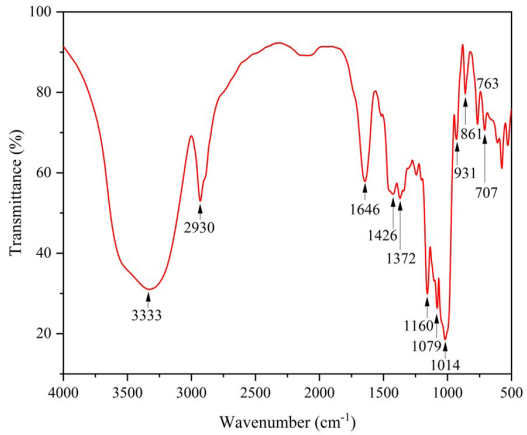

Figure 3. FTIR spectrum of BM was investigated in the 4000−500 cm^{-1} region.

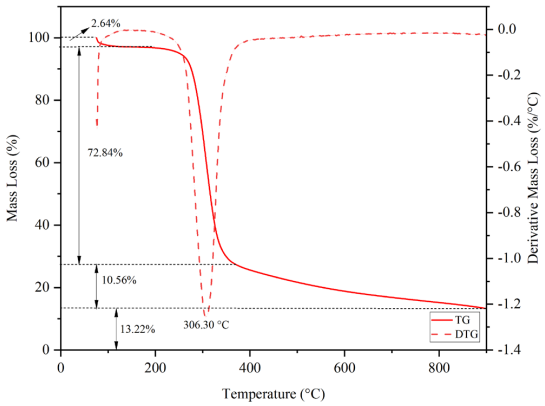

Figure 4. TG and DTG curves of BM and the corresponding thermal events.

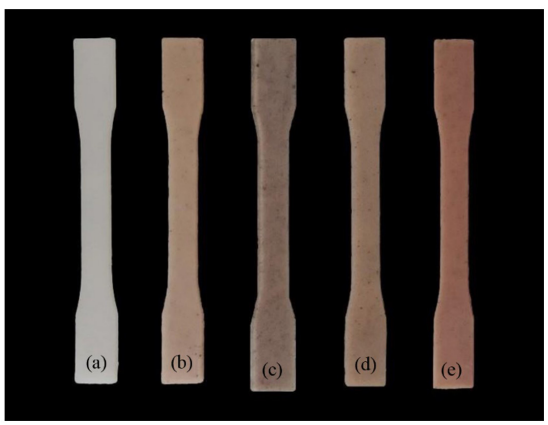

Figure 5. Macroscopic analysis performed for (a) Bio-PE, (b) Bio-PE/1.5BM, (c) Bio-PE/3BM, (d) Bio-PE/1.5BM/3PE-*g*-MA, and (e) Bio-PE/3BM/3PE-*g*-MA.

All composites were produced using injection molding, resulting in a satisfactory finish and uniform color. However, small agglomerates appeared in some areas due to physical interactions between particles. The incorporation of BM particles significantly affected the composite color, changing from the white of neat Bio-PE to a brownish hue, which darkened as the BM content increased from 1.5 to 3 wt%. Composites with PE-*g*-MA in the formulation exhibited a better surface finish and more uniform color, indicating that the compatibilizer improved wettability and the interfacial bond between the polymer and the filler. Rojas-Lema et al.[5] observed similar results in Bio-PE/Persimmon Peel Flour/PE-*g*-MA composites.

3.4 Optical Microscopy (OM)

Optical microscopy was employed to preliminarily assess the distribution and dispersion of BM particles in Bio-PE, as these factors significantly influence the material's mechanical properties. Figure 6 illustrates the surface micrographs of the specimens.

None of the specimens exhibited visible bubbles or pores, indicating minimal surface defects. The Bio-PE-based specimen (Figure 6e) presented a more uniform appearance compared to the composites, which showed particle agglomeration increasing with filler content, especially in the absence of PE-*g*-MA (Figure 6a-b). This agglomeration is partly attributed to the low density of BM particles, which complicates manual pre-mixing.

The incorporation of PE-*g*-MA (Figure 6.c-d) reduced agglomerates and improved dispersion, although some clusters remained, indicating the need for further processing optimization. The use of a single-screw extruder may have limited shear and mixing efficiency[22]. The disparity in surface energy between the filler and the polymer matrix favors particle coalescence, resulting in small agglomerates. These act as stress concentrators, weakening the mechanical properties under stress[11]. Achieving homogeneous dispersion is essential to maximize the effectiveness of reinforcement.

3.5 Contact Angle (θ)

The contact angle measures the interaction between a surface and a liquid, indicating whether a surface is hydrophilic or hydrophobic. Surfaces are classified as super hydrophilic ($\theta < 10°$), hydrophilic ($\theta \leq 90°$), hydrophobic ($90° < \theta \leq 150°$), or superhydrophobic ($150° < \theta \leq 180°$) [23]. Table 2 presents the average contact angle values and droplet images.

The Bio-PE formulation exhibited a contact angle of approximately 86.15°, indicating a hydrophilic surface due to some polar component originating from its synthesis. Similar results were reported by Bezerra et al.[4] and Jorda-Reolid et al.[6], who observed contact angles below 90° for neat Bio-PE, attributed to the presence of residual polar groups and processing agents. Incorporating BM into Bio-PE resulted in a significant reduction in the contact angle, specifically by 2.75% for the Bio-PE/1.5BM and by 4.20% for the Bio-PE/3BM composite, demonstrating increased hydrophilicity. This enhancement is attributed to the numerous free hydroxyl groups in the BM, which increase hydrophilicity despite the relatively low amount of mesocarp in the composites.

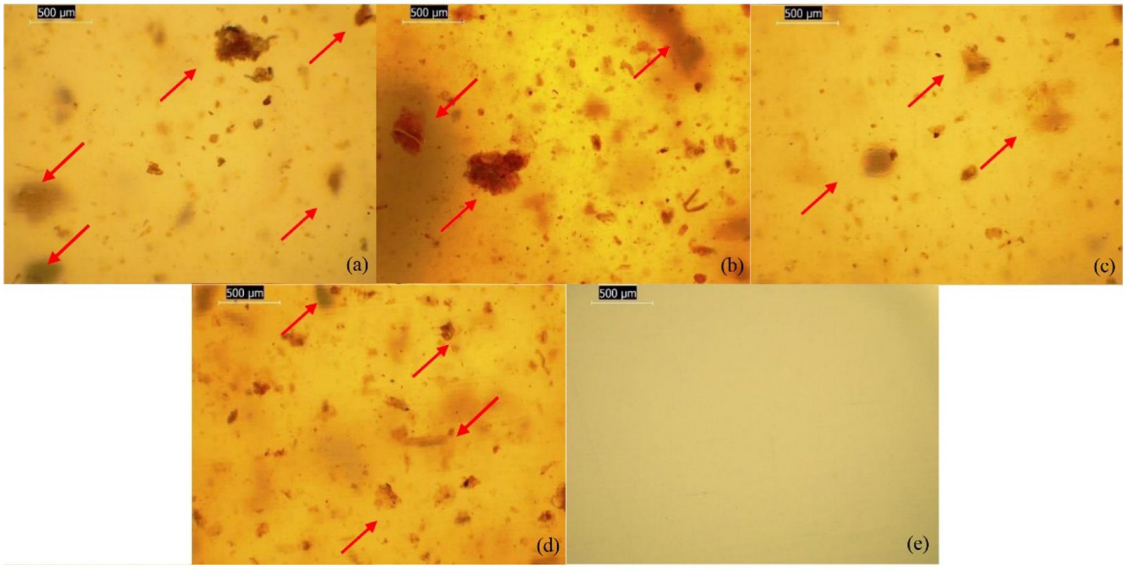

Figure 6. Surface micrographs obtained by OM of (a) Bio-PE/1.5BM, (b) Bio-PE/3BM, (c) Bio-PE/1.5BM/3PE-*g*-MA, (d) Bio-PE/3BM/3PE-*g*-MA, and (e) Bio-PE (40x/500 µm).

Table 2. Average contact angle value and the water droplet image.

Formulations	Contact Angle (°)	
	Average value	Water droplet image
Bio-PE	$86.15^{a} \pm 1.17$	
Bio-PE/1.5BM	$83.80^{b} \pm 0.99$	
Bio-PE/3BM	$82.54^{b} \pm 1.24$	
Bio-PE/1.5BM/3PE-*g*-MA	$89.70^{c} \pm 1.29$	
Bio-PE/3BM/3PE-*g*-MA	$90.76^{c} \pm 1.96$	

Data were expressed as means ± standard deviation ($n = 10$). Means with different letters within the same column represent statistically significant differences by the Tukey test ($p < 0.05$).

Incorporating PE-*g*-MA into the formulation significantly increased the contact angle, with a 6.58% rise for Bio-PE/1.5BM/3PE-*g*-MA and a 9.06% rise for Bio-PE/3BM/3PE-*g*-MA compared to composites without the compatibilizer. This improvement is attributed to the interaction between the maleic anhydride groups in PE-*g*-MA and the hydroxyl groups on plant fillers, such as BM. This interaction reduces the free hydroxyl groups available for interacting with water, enhancing surface hydrophobicity. Additionally, the long PE chains in PE-*g*-MA further contribute to hydrophobicity by diffusing into the polymer. These findings align with the results of manuscripts published by other authors on composites containing PE-*g*-MA[6,12].

3.6 Tensile strength test

The tensile strength test is a key method in materials science for assessing mechanical properties, including polymers' response to stress and strain. Table 3 and Figure 7 data are crucial for practical material design and engineering applications.

Figure 7 presents stress–strain curves and images of specimens following a tensile strength test. The Bio-PE exhibited ductile behavior, characterized by significant deformation without fracture. This behavior is likely due to its long molecular chains and high molecular weight, contributing to its resilience and flexibility. The Bio-PE chains rearranged during the tensile test, facilitating substantial plastic deformation without fracturing. The tensile strength was comparable between the neat polymer and the composites. However, the maximum deformation decreased with the BM incorporation, particularly in the Bio-PE/3BM and Bio-PE/3BM/3PE-*g*-MA composites, which exhibited brittle behavior. This reduction is attributed to a possible incompatibility between the BM and Bio-PE, consistent with other research[2,3].

The reduced deformation observed in composites with 3 wt%, compared to those with 1.5 wt%, is attributable to the particles acting as barriers to polymer chain movement and as stress concentrators. This interference leads to earlier fracture under tension. PE-*g*-MA improved deformation by 76.49% in the Bio-PE/1.5BM/3PE-*g*-MA composite (51.50%) compared to the Bio-PE/1.5BM composite (12.11%). However, this benefit did not extend to composites with 3 wt% due to agglomeration, which impaired particle distribution and stress transfer within the polymer matrix[11].

Table 3. Mechanical properties obtained from the tensile strength test.

Formulations	Tensile Strength Properties (MPa)		
	Yield Stress	Ultimate Tensile Strength	Young's Modulus
Bio-PE	$9.34^{a} \pm 0.44$	NB	$364.88^{a} \pm 9.29$
Bio-PE/1.5BM	$7.72^{b} \pm 0.68$	$2.38^{a} \pm 0.19$	$316.84^{b} \pm 7.90$
Bio-PE/3BM	$10.78^{c} \pm 0.51$	$10.36^{b} \pm 0.62$	$292.66^{c} \pm 15.72$
Bio-PE/1.5BM/3PE-*g*-MA	$10.74^{c} \pm 0.50$	$3.46^{a} \pm 0.23$	$377.64^{a} \pm 12.19$
Bio-PE/3BM/3PE-*g*-MA	$13.48^{d} \pm 0.94$	$20.52^{c} \pm 1.19$	$362.22^{a} \pm 10.05$

NB – No break. Data were expressed as means ± standard deviation (n = 5). Means with different letters within the same column represent statistically significant differences by the Tukey test ($p < 0.05$).

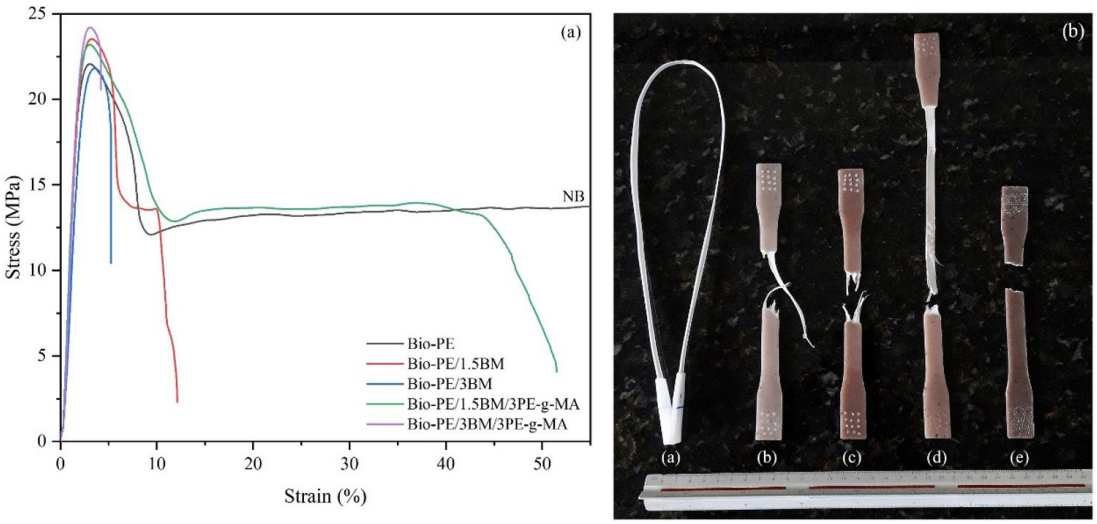

Figure 7. Scheme illustrating (a) the stress–strain curves of Bio-PE and its composites, and (b) the specimens after the tensile strength test: (a) Bio-PE, (b) Bio-PE/1.5BM, (c) Bio-PE/3BM, (d) Bio-PE/1.5BM/3PE-*g*-MA, and (e) Bio-PE/3BM/3PE-*g*-MA.

Table 3 reveals a 17.34% reduction in yield stress for the Bio-PE/1.5BM composite compared to Bio-PE, attributed to stress concentration from particles that may accelerate crack propagation[1]. Conversely, the yield stress increased by 13.36% for the Bio-PE/3BM composite, by 13.06% for the Bio-PE/1.5BM/3PE-*g*-MA composite, and by 30.71% for the Bio-PE/3BM/3PE-*g*-MA composite. PE-*g*-MA improved the interfacial adhesion between the filler and the polymer matrix by interacting with the hydroxyl groups of BM. This interaction enhanced stress transfer and increased the composite's resistance[3].

The Bio-PE specimen did not exhibit ultimate tensile strength because it did not fracture, owing to its significant plastic deformation capacity. Among the composites, Bio-PE/1.5BM and Bio-PE/1.5BM/3PE-*g*-MA exhibited similar ultimate tensile strengths due to the absence of fracture in Bio-PE. However, Bio-PE/3BM/3PE-*g*-MA demonstrated a 50.49% increase in ultimate tensile strength compared to Bio-PE/3BM. This enhancement is attributed to the reinforcing effect of the compatibilizer, which improves the interaction between Bio-PE and BM. During processing, part of the PE-*g*-MA migrates to the matrix–filler interface, where its anhydride groups react with hydroxyl groups in the BM. This chemical interaction enhances interfacial adhesion, facilitating stress transfer from the matrix to the filler and improving the mechanical strength of the composite[14].

Incorporating BM into Bio-PE resulted in a 13.17% reduction in Young's modulus for Bio-PE/1.5BM and a 19.79% reduction for Bio-PE/3BM. This reduction may be due to the presence of residual natural components in the BM, such as lipids or waxes, which can act as plasticizing agents and interfere with the rigidity and interfacial bonding of the composite[17]. However, the addition of PE-*g*-MA restored the modulus, suggesting that the compatibilizer enhanced the interaction between the polymer matrix and the dispersed particles, resulting in more efficient stress transfer. The restoration of the modulus can be attributed to localized interfacial interactions between Bio-PE and BM, promoted by PE-*g*-MA, which enhanced load transfer despite the non-uniform dispersion of the particles. PE-*g*-MA may have reduced the incompatibility between the phases, minimizing interfacial defects that could compromise the material's rigidity[3,6].

3.7 Izod impact strength

Impact strength is critical for polymers, as they often fail under sudden loads. Table 4 shows the results of the Izod test, which measured this property.

The analysis of Izod impact resistance results showed that the inclusion of BM, whether alone or in combination with PE-*g*-MA, did not result in statistically significant

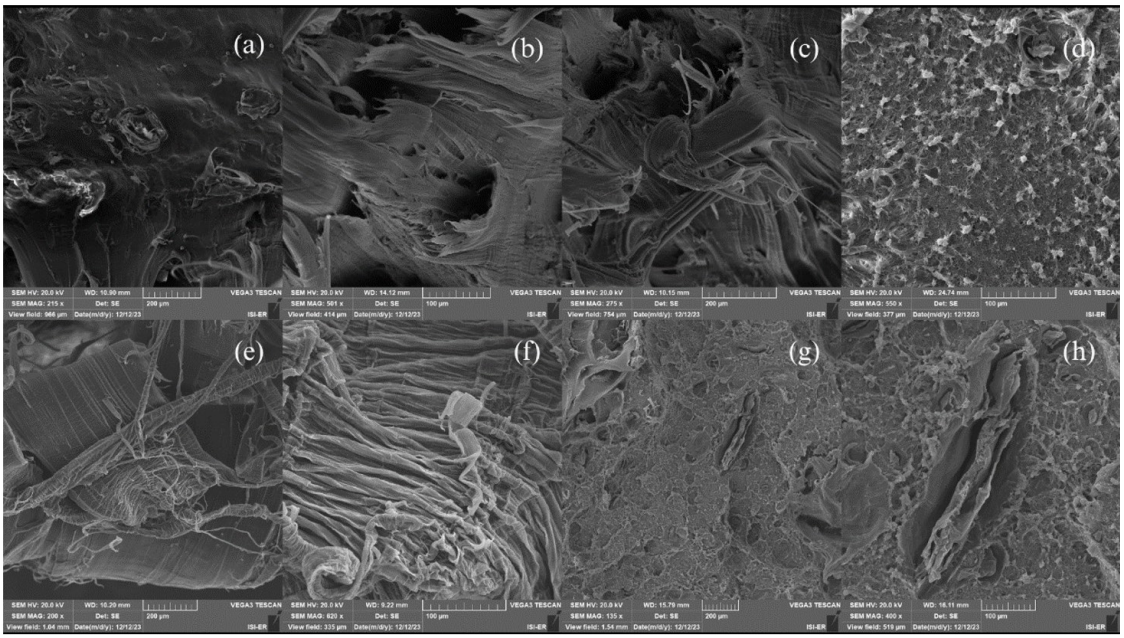

Figure 8. Fracture surface morphology: (a-b) Bio-PE/1.5BM, (c-d) Bio-PE/3BM, (e-f) Bio-PE/1.5BM/3PE-*g*-MA, and (g-h) Bio-PE/3BM/3PE-*g*-MA (200-100 μm scale).

Table 4. Data obtained from the impact strength test for composites based on Bio-PE/BM.

Formulations	Izod Impact Strength (J/m)
Bio-PE	48.77^{a} ± 0.30
Bio-PE/1.5BM	48.55^{a} ± 0.26
Bio-PE/3BM	48.97^{a} ± 0.11
Bio-PE/1.5BM/3PE-*g*-MA	48.83^{a} ± 0.14
Bio-PE/3BM/3PE-*g*-MA	48.89^{a} ± 0.25

Data were expressed as means ± standard deviation (n = 5). Means with different letters within the same column represent statistically significant differences by the Tukey test ($p < 0.05$).

changes in Bio-PE/BM composites compared to pure Bio-PE, as evidenced by the Tukey test ($p < 0.05$). Pure Bio-PE exhibited an average impact resistance of 48.77 J/m, while formulations containing 1.5 and 3 wt% of BM, with or without PE-*g*-MA, showed minimal variations, maintaining values close to the control. This behavior indicates that the inclusion of BM does not affect the material's energy dissipation in response to impact, even with its reduced dispersion in the polymer matrix[22]. Additionally, the presence of PE-*g*-MA compatibilizer also did not influence impact resistance, suggesting that, despite its ability to enhance the interaction between BM and the polymer matrix, its action was not effective in altering fracture propagation properties[3].

3.8 Scanning Electron Microscopy (SEM)

SEM reveals the composite's internal structure and fracture details after the tensile strength test, highlighting the interaction between the Bio-PE and the BM particles, which impact the mechanical properties, according to Figure 8. The fracture surface morphology of neat Bio-PE was not analyzed due to the absence of a fracture. The Bio-PE/1.5BM composite exhibited ductile fracture behavior, with visible plastic deformation, resulting in an irregular, wavy surface with signs of tearing (Figure 8.a-b). The Bio-PE/3BM composite also displayed ductile fracture characteristics but with a rougher surface and indications of less plastic deformation (Figure 8.c-d), suggesting a transition to a more brittle behavior. In Figure 8.d, structural defects, such as voids, valleys, and microcracks, can be observed, acting as stress concentrators[2,5].

The incorporation of PE-*g*-MA significantly influenced the fracture surface morphology of the composites. A fibrous pattern emerged in the Bio-PE/1.5BM/3PE-*g*-MA (Figure 8e-f), indicating extensive plastic deformation and energy absorption. This observation suggested that the polymer chains had aligned and stretched, forming fibrils under stress[1]. In contrast, the Bio-PE/3BM/3PE-*g*-MA (Figure 8.g-h) displayed a more irregular and rough morphology, suggesting shallow deformation and rapid crack propagation due to weak adhesion between phases, which compromised stress transfer and reduced ductility[3].

3.9 Water absorption

The water absorption test evaluated how moisture affected the strength and stability. Figure 9 and Table S1 (Supplementary Material) display the results at three temperatures.

The research found that water absorption in composites increased over time, with Bio-PE demonstrating superior moisture resistance and lower water absorption. This reduced absorption in Bio-PE is attributed to its non-polar nature and tightly packed polymer chains, which impede water penetration. The absence of polar functional groups

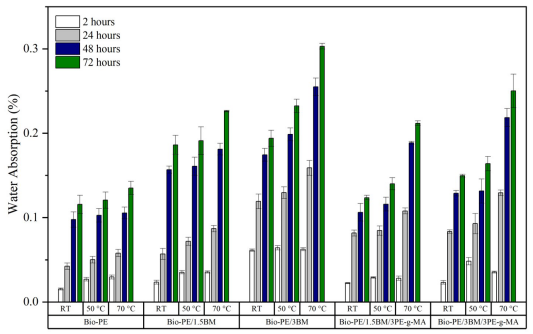

Figure 9. Water absorption under varying conditions of time and temperature.

enhances Bio-PE's hydrophobic properties. A higher BM content in the composites resulted in increased water absorption, except for the Bio-PE/1.5BM composite at RT for 24 h, which exhibited water absorption similar to that of pure Bio-PE. Similarly, the Bio-PE/3BM composite did not differ significantly from the Bio-PE/1.5BM composite at 48 and 72 h. The increased water absorption in the composites is attributed to the polar hydroxyl groups in BM, which attract water molecules through hydrogen bonds, forming a hydration layer.

The Bio-PE/3BM/3PE-*g*-MA exhibited a reduction in water absorption, whereas the Bio-PE/1.5BM/3PE-*g*-MA did not differ significantly from the Bio-PE/1.5BM. This reduction in water absorption, which ranged from 14.90 to 33.57% over 72 h, is attributed to the improved interaction and adhesion between Bio-PE and BM, which likely minimized voids at the interface and thereby reduced water retention. The PE-*g*-MA component decreased the composite's polarity, lowering its water affinity. A manuscript by Panthapulakkal and Sain[24] found that a compatibilizing agent reduced water absorption in HDPE-based composites by minimizing flaws at the matrix/filler interface. However, increased temperature resulted in higher water absorption, ranging from 8.72 to 35.99%, due to decreased water density and viscosity and increased polymer chain mobility, facilitating water penetration[25].

4. Conclusions

The BM characterization showed it has a chemical structure similar to starch and high thermal stability, with significant degradation only above 200 °C. In composites, injection molding resulted in a well-finished product with well-distributed particles, although some agglomerates affected wettability. Adding PE-*g*-MA at 1.5 wt% improved plastic deformation. BM content and PE-*g*-MA usage variations influenced tensile strength, while impact strength remained unchanged. Analyzing the fracture surface using SEM provided insights into the composite's behavior. BM particles increased water absorption, but PE-*g*-MA mitigated this effect. The research highlighted the BM potential and value in producing green composites, aligning with ecological and circular economy principles.

5. Author's Contribution

- **Conceptualization –** Crisnam Kariny da Silva Veloso; Renata Barbosa.
- **Data curation –** Crisnam Kariny da Silva Veloso.
- **Formal analysis –** Crisnam Kariny da Silva Veloso.
- **Funding acquisition –** NA.
- **Investigation –** Crisnam Kariny da Silva Veloso.
- **Methodology –** Crisnam Kariny da Silva Veloso; Renata Barbosa.
- **Project administration –** Renata Barbosa.
- **Resources –** Renata Barbosa; Tatianny Soares Alves; Ruth Marlene Campomanes Santana.
- **Software –** NA.
- **Supervision –** Renata Barbosa; Tatianny Soares Alves.
- **Validation –** Crisnam Kariny da Silva Veloso; Renata Barbosa.
- **Visualization –** Crisnam Kariny da Silva Veloso.
- **Writing – original draft –** Crisnam Kariny da Silva Veloso; Lucas Rafael Carneiro da Silva.
- **Writing – review & editing –** Crisnam Kariny da Silva Veloso; Lucas Rafael Carneiro da Silva; Renata Barbosa.

6. Acknowledgements

The authors want to acknowledge the Federal University of Piauí (UFPI), Postgraduate Program in Materials Science and Engineering (PPGCM), Piauí State Research Support Foundation (FAPEPI) [EDITAL FAPEPI/MCTIC/CNPq Nº 008/2018], National Council for Scientific and Technological Development (CNPq), and Coordination for the Improvement of Higher Education Personnel (CAPES).

7. References

1. Essabir, H., Bensalah, M. O., Rodrigue, D., Bouhfid, R., & Qaiss, A. E. K. (2016). Biocomposites based on Argan nut shell and a polymer matrix: effect of filler content and coupling agent. *Carbohydrate Polymers*, *143*, 70-83. http://doi.org/10.1016/j.carbpol.2016.02.002. PMid:27083345.
2. Rodríguez, L. J., Álvarez-Láinez, M. L., & Orrego, C. E. (2022). Optimization of processing conditions and mechanical properties of banana fiber-reinforced polylactic acid/high-density polyethylene biocomposites. *Journal of Applied Polymer Science*, *139*(3), 51501. http://doi.org/10.1002/app.51501.
3. Dolza, C., Fages, E., Gonga, E., Gomez-Caturla, J., Balart, R., & Quiles-Carrillo, L. (2021). Development and characterization of environmentally friendly wood plastic composites from biobased polyethylene and short natural fibers processed by injection moulding. *Polymers*, *13*(11), 1692. http://doi.org/10.3390/polym13111692. PMid:34067283.
4. Bezerra, E. B., França, D. C., Morais, D. D. S., Silva, I. D. S., Siqueira, D. D., Araújo, E. M., & Wellen, R. M. R. (2019). Compatibility and characterization of Bio-PE/PCL blends. *Polímeros*, *29*(2), e2019022. http://doi.org/10.1590/0104-1428.02518.
5. Rojas-Lema, S., Lascano, D., Ivorra-Martinez, J., Gomez-Caturla, J., Balart, R., & Garcia-Garcia, D. (2021). Manufacturing and characterization of high-density polyethylene composites

with active fillers from persimmon peel flour with improved antioxidant activity and hydrophobicity. *Macromolecular Materials and Engineering*, *306*(11), 2100430. http://doi.org/10.1002/mame.202100430.

6. Jorda-Reolid, M., Gomez-Caturla, J., Ivorra-Martinez, J., Stefani, P. M., Rojas-Lema, S., & Quiles-Carrillo, L. (2021). Upgrading argan shell wastes in wood plastic composites with biobased polyethylene matrix and different compatibilizers. *Polymers*, *13*(6), 922. http://doi.org/10.3390/polym13060922. PMid:33802815.
7. Moshood, T. D., Nawanir, G., Mahmud, F., Mohamad, F., Ahmad, M. H., & AbdulGhani, A. (2022). Sustainability of biodegradable plastics: new problem or solution to solve the global plastic pollution? *Current Research in Green and Sustainable Chemistry*, *5*, 100273. http://doi.org/10.1016/j.crgsc.2022.100273.
8. Spierling, S., Knüpffer, E., Behnsen, H., Mudersbach, M., Krieg, H., Springer, S., Albrecht, S., Herrmann, C., & Endres, H.-J. (2018). Bio-based plastics: a review of environmental, social, and economic impact assessments. *Journal of Cleaner Production*, *185*, 476-491. http://doi.org/10.1016/j.jclepro.2018.03.014.
9. González-Pérez, S. E., Coelho-Ferreira, M., Robert, P., & Garcés, C. L. L. (2012). Conhecimento e usos do babaçu (*Attalea speciosa* Mart. e *Attalea eichleri* (Drude) A. J. Hend.) entre os Mebêngôkre-Kayapó da Terra Indígena Las Casas, estado do Pará, Brasil. *Acta Botanica Brasílica*, *26*(2), 295-308. http://doi.org/10.1590/S0102-33062012000200007.
10. Silva, L. R. C., Alves, T. S., Barbosa, R., Morisso, F. D. P., Rios, A. O., & Santana, R. M. C. (2023). Characterization of babassu mesocarp flour as potential bio-reinforcement for poly(lactic acid). *Journal of Food Industry*, *7*(1), 24-53. http://doi.org/10.5296/jfi.v7i1.21066.
11. Silva, N. F. I., Soares, J. E., Fo., Santos, T. G. C., Chagas, J. S., Medeiros, S. A. S. L., Santos, E. B. C., Wellen, R. M. R., Silva, L. B., Carvalho, L., Nunes, M. A. B. S., & Santos, A. S. F. (2021). Biocomposites based on poly(hydroxybutyrate) and the mesocarp of babassu coconut (*Orbignya phalerata Mart.*): effect of wax removal and maleic anhydride-modified polyethylene addition. *Journal of Materials Research and Technology*, *15*, 3161-3170. http://doi.org/10.1016/j.jmrt.2021.09.008.
12. Maniglia, B. C., Tessaro, L., Lucas, A. A., & Tapia-Blácido, D. R. (2017). Bioactive films based on babassu mesocarp flour and starch. *Food Hydrocolloids*, *70*, 383-391. http://doi.org/10.1016/j.foodhyd.2017.04.022.
13. Alim, A. A. A., Baharum, A., Shirajuddin, S. S. M., & Anuar, F. H. (2023). Blending of Low-Density Polyethylene and Poly(Butylene Succinate) (LDPE/PBS) with Polyethylene–Graft–Maleic Anhydride (PE–g–MA) as a compatibilizer on the phase morphology, mechanical and thermal properties. *Polymers*, *15*(2), 261. http://doi.org/10.3390/polym15020261. PMid:36679142.
14. Prajapati, R. S., Jain, S., & Shit, S. C. (2017). Development of basalt fiber-reinforced thermoplastic composites and effect of PE-g-MA on composites. *Polymer Composites*, *38*(12), 2798-2805. http://doi.org/10.1002/pc.23879.
15. Bal, T., Yadav, S. K., Rai, N., Swain, S., Shambhavi, Garg, S., & Sen, G. (2020). Invitro evaluations of free radical assisted microwave irradiated polyacrylamide grafted cashew gum (CG) biocompatible graft copolymer (CG-g-PAM) as effective polymeric scaffold. *Journal of Drug Delivery Science and Technology*, *56*(Pt A), 101572. http://doi.org/10.1016/j.jddst.2020.101572.
16. Greene, J. P. (2021). *Microstructures of polymers.* In J. P. Greene. *Automotive plastics and composites* (pp. 27-37). Norwich: William Andrew Publishing. http://doi.org/10.1016/B978-0-12-818008-2.00009-X.
17. Vu, H. P. N., & Lumdubwong, N. (2016). Starch behaviors and mechanical properties of starch blend films with different plasticizers. *Carbohydrate Polymers*, *154*, 112-120. http://doi.org/10.1016/j.carbpol.2016.08.034. PMid:27577902.
18. Thivya, P., Bhosale, Y. K., Anandakumar, S., Hema, V., & Sinija, V. R. (2021). Exploring the effective utilization of shallot stalk waste and tamarind seed for packaging film preparation. *Waste and Biomass Valorization*, *12*(10), 5779-5794. http://doi.org/10.1007/s12649-021-01402-4.
19. Abdullah, A. H. D., Chalimah, S., Primadona, I., & Hanantyo, M. H. G. (2018). Physical and chemical properties of corn, cassava, and potato starchs. *IOP Conference Series: Earth and Environmental Science*, *160*, 012003. http://doi.org/10.1088/1755-1315/160/1/012003.
20. Singh, R., Kaur, S., & Aggarwal, P. (2021). Exploration of potato starches from non-commercial cultivars in ready to cook instant non cereal, non glutinous pudding mix. *Lebensmittel-Wissenschaft + Technologie*, *150*, 111966. http://doi.org/10.1016/j.lwt.2021.111966.
21. Edvan, R., Sá, M., Magalhães, R., Ratke, R., Sousa, H. R., Neri, L. M. L., Silva-Filho, E. C., Pereira, J., Fo., & Bezerra, L. (2020). Copolymerized natural fibre from the mesocarp of orbignya phalerata (babassu fruit) as an irrigating-fertilizer for growing cactus pears. *Polymers*, *12*(8), 1699. http://doi.org/10.3390/polym12081699. PMid:32751245.
22. Barbos, J. D. V., Azevedo, J. B., Cardoso, P. S. M., Garcia, F. C., Fo., & del Río, T. G. (2020). Development and characterization of WPCs produced with high amount of wood residue. *Journal of Materials Research and Technology*, *9*(5), 9684-9690. http://doi.org/10.1016/j.jmrt.2020.06.073.
23. Ahmad, D., van den Boogaert, I., Miller, J., Presswell, R., & Jouhara, H. (2018). Hydrophilic and hydrophobic materials and their applications. *Energy Sources. Part A, Recovery, Utilization, and Environmental Effects*, *40*(22), 2686-2725. http://doi.org/10.1080/15567036.2018.1511642.
24. Panthapulakkal, S., & Sain, M. (2007). Agro-residue reinforced high-density polyethylene composites: fiber characterization and analysis of composite properties. *Composites. Part A, Applied Science and Manufacturing*, *38*(6), 1445-1454. http://doi.org/10.1016/j.compositesa.2007.01.015.
25. Chen, R. S., Ab Ghani, M. H., Salleh, M. N., Ahmad, S., & Tarawneh, M. A. A. (2015). Mechanical, water absorption, and morphology of recycled polymer blend rice husk flour biocomposites. *Journal of Applied Polymer Science*, *132*(8), 41494. http://doi.org/10.1002/app.41494.

Received: Aug. 29, 2024
Revised: Apr. 23, 2025
Accepted: May 24, 2025

Associate Editor: José A. C. G. Covas

Supplementary Material

Supplementary material accompanies this paper.

Table S1. Data obtained from the water absorption test for Bio-PE and composites based on Bio-PE/BM.

This material is available as part of the online article from https://doi.org/10.1590/0104-1428.20240084